Dolomite Decomposition to (Ca,Mg)O Solid Solutions: An X-Ray Diffraction Study, Part I.

G. Spinolo and U. Anselmi Tamburini
Dipartimento di Chimica Fisica dell'Universita, and Centro di studi per la Termodinamica ed Elettrochimica dei sistemi salini fusi e solidi del C.N.R. viale Taramelli, 16, I-27100 Pavia (Italy)

Z. Naturforsch. **39a,** 975–980 (1984); received July 24, 1984

Dolomite [$CaMg(CO_3)_2$] full decomposition has been studied by *in situ* powder X-ray diffraction. The primary products are Ca-rich and Mg-rich (Ca,Mg)O solid solutions with compositions different from equilibrium values. In some cases a strained form of calcite is also produced. The experimental results show that the oxides are formed in a direct process with a shear mechanism, whereas calcite formation is due to CaO recarbonation.

It is well known that dolomite, the ordered solution of calcium and magnesium carbonates, decomposes either to produce calcite, periclase and carbon dioxide ("half decomposition"):

$$CaMg(CO_3)_2 \rightarrow CaCO_3 + MgO + CO_2 \qquad (1)$$

or to produce lime, periclase and carbon dioxide ("full decomposition"):

$$CaMg(CO_3)_2 \rightarrow CaO + MgO + 2\,CO_2\,. \qquad (2)$$

The equilibrium relationships between the various phases have been stated in a previous paper [1] through a thermodynamic analysis based on a subregular model for the calcite-magnesite solid solutions, on the experimental data available for the $Ca,Mg/CO_3$ pseudobinary system, and on some simplifying assumptions. It turns out that for each temperature there is a threshold CO_2 pressure. Below this critical value the equilibrium is described by (2); above it only the half decomposition takes place, although in a way slightly different from (1): a magnesian calcite is produced and its Mg content depends on the partial CO_2 pressure.

This analysis gives also some insight into the kinetics of reactions (1) and (2), allowing one to discard some of the mechanisms suggested previously. However, it does not provide a definitive choice because other factors, such as the amount of strains connected with the structural rearrangements, and the local carbon dioxide pressure at the reaction interface may favour one or another of the possible mechanisms.

Reprint requests to Prof. Giorgio Spinolo, Dipartimento di Chimica Fisica dell'Universita, Viale Taramelli, 16. I-27100 Pavia (Italy).

It must be noted that the half decomposition has received much more attention than the full decomposition. For the latter, little is known except for a combined torsion-effusion and torsion-Langmuir study by Powell and Searcy [2]: it shows that highly disordered and metastable ("glasslike") solids are formed through a complex process (which includes an irreversible step), and that carbon dioxide desorption is not rate-limiting.

In close connection with Powell and Searcy's paper, we report here on an X-Ray powder diffraction study of dolomite decomposition in high vacuum, *viz.*, at partial carbon dioxide pressures much lower than the equilibrium value for full decomposition. The primary aim of this work is to investigate the mechanism of dolomite full decomposition by monitoring directly the solid phases during the reaction, but we think that the measurements may also help in solving a more general problem.

For a number of reasons, alkaline earth carbonates, as well as hydroxides, are probably the chemical model most frequently used to study endothermic decomposition reactions of the type

$$AB(solid) \rightarrow A(solid) + B(gas)$$

and, particularly, the relations between thermodynamics, kinetics and microstructure. In the last ten years some experimental facts have been investigated with a particular emphasis, among which:

i) the nature of the so-called "special reactivity" oxides [3], *i.e.*, of materials characterized by a very large reactivity towards liquids and gases, by an anomalously great thermodynamic activity, and by

0340-4811 / 84 / 1000-0975 $ 01.30/0. – Please order a reprint rather than making your own copy.

a highly porous microstructure made of small crystallites bound together into boundles which keep the shape of the original particles of the parent product, and

ii) the conflicting relevance of two different processes suggested for the interface advancement [4], *i.e.*, a diffusional process (like that of the nucleation-and-growth mechanism), and a diffusionless shear mechanism (like that of martensitic transformations).

In dolomite decomposition two formal processes occur, *i.e.*, the "chemical" decomposition and the unmixing of a homogeneous solution of two different cations. Using an experimental technique which detects directly the solid phases, we can follow both processes. This fact, together with a knowledge of the thermodynamics of the system, may potentially give the best information about the underlying mechanisms of endothermic decomposition reactions.

Experimental

X-Ray powder diffraction (XRD) patterns were taken with a Philips diffractometer (PW 1730 generator, PW 1050 goniometer, PW 1390 channel control, PW 1394 motor control, PW 1395 programmer) equipped with a proportional counter, a copper tube (wavelength = 0.15418 nm) operated at 45 kV and 22 mA, and a home-made environmental chamber [5].

Two different procedures were used to record the powder patterns. Most of the measurements were made with the usual continuous scan method with ratemeter and chart recorder, but in some cases the step scan method was preferred. In the latter case a Victor 9000 microcomputer was connected to the serial interface of the channel control unit. A series of home developed programs [6] was used: (i) to build up and send the step scan commands for the programmer unit, (ii) to receive and store on floppy disc files the raw (angle-counts-time) data, (iii) to produce the final data by summing up the raw data of the various scans, and (iv) to display the diffractogram on the CRT screen and on a dot matrix printer.

A three action thermoregulator, connected with a recorder and with a thermocouple type K, was used to drive the furnace surrounding the nickel block acting as the specimen holder; precise temperature measurements were made with a different thermocouple placed within the block very close to the sample.

The vacuum, produced by an oil diffusion pump provided with a liquid nitrogen trap, was measured by a Penning gauge head placed in front of the sample surface.

For each decomposition run, the furnace temperature was raised stepwise, under vacuum, and stopped at some 50 K below the decomposition onset, to outgas the environmental chamber. Then, the temperature was once more raised, as quickly as possible, but preventing the sample to overheat by more than a few kelvins. This last heating never took more than ten minutes, including the time needed to stabilize the temperature close to the preset value.

A series of complete diffractograms (in the range $20-50°$, $2\varnothing$) was made: (i) immediately after the final temperature had been reached, (ii) when the reaction was almost complete, and (iii) at several intermediate times during decomposition, using either continuous scan or step scan. In the latter case the following procedure was adopted to take each of the diffractograms: (i) the decomposition reaction was interrupted by breaking the furnace power, (ii) the sample was allowed to cool overnight under vacuum down to room temperature, (iii) the XRD pattern was step scan recorded, and (iv) the temperature was raised again to the previous value. With this rather complicate step scan procedure a much longer recording time could be used so that it was possible to detect with a greater accuracy some small details of the patterns, but we usually preferred the simpler continuous scan method which does not need to stop decomposition. Note that the time needed to record a complete pattern with continuous scan (less than one hour) can be considered small compared to the overall reaction time (always longer than two days). In either case, the temperature values and their accuracies, reported in the following for each decomposition experiment, give the averages and the standard errors over the whole reaction time.

The dolomite sample was kindly supplied by Alan W. Searcy (University of California-Berkeley and Lawrence Berkeley Laboratory) and belongs to the same batch used for the already mentioned study [3]: it is in the form of transparent light yellow single crystals from Pamplona (Spain), and contains

some iron (mole fraction: ~ 0.01). After grinding and sieving, the 5–50 μm fraction was used.

We report hereafter the details of the various experiments.

Experiment A: decomposition temperature (850.2 ± 1.5) K; maximum decomposition pressure $< 10^{-3}$ Torr ($\sim 1.3\ 10^{-1}$ Pa); the reaction was almost complete after 50 h; the pertinent XRD patterns are designed as A-0, ..., A-50 (each figure meaning the mean reaction time correspondent to a given pattern).

Experiment B: decomposition temperature (792.2 ± 0.7) K; maximum decomposition pressure $< 10^{-3}$ Torr ($\sim 1.3\ 10^{-1}$ Pa); XRD patterns: B-0 to B-130 (the last pattern was taken at room temperature with step scan). The reaction was almost complete after 130 h; the sample was then transferred into an open air furnace and heated at 1000 K for several days; a new pattern (B-F; F = final) was finally taken at room temperature.

Experiment C: decomposition temperature (849 ± 3) K; maximum decomposition pressure $< 10^{-4}$ Torr ($\sim 1.3\ 10^{-2}$ Pa); XRD patterns were taken with step scan after 150 min (C-2.5), after 25 h (C-25), and after 50 h (C-50).

Results

Figure 1 shows a typical XRD pattern of reaction products (almost complete decomposition, pattern B-130): we can see the diffraction lines of lime and periclase, a few calcite lines, and the strongest dolomite line due to the last amount of unreacted reagent, as well as lines of the nickel sample holder and of some unidentified impurity.

In all experiments, the main products of decomposition were lime and periclase, *i.e.* CaO and MgO

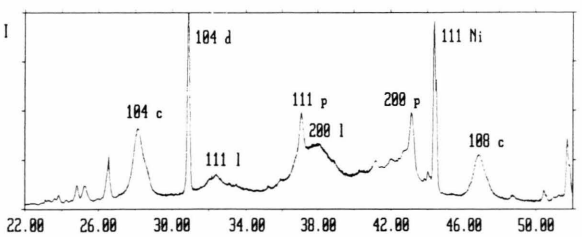

Fig. 1. Powder XRD pattern B-130, taken close to the end of decomposition run B ($T = 792$ K). The diffraction lines of lime (l), periclase (p), calcite (c), as well as those of the last residues of dolomite (d) and of the (Ni) sample holder are indicated together with their crystallographic indexes.

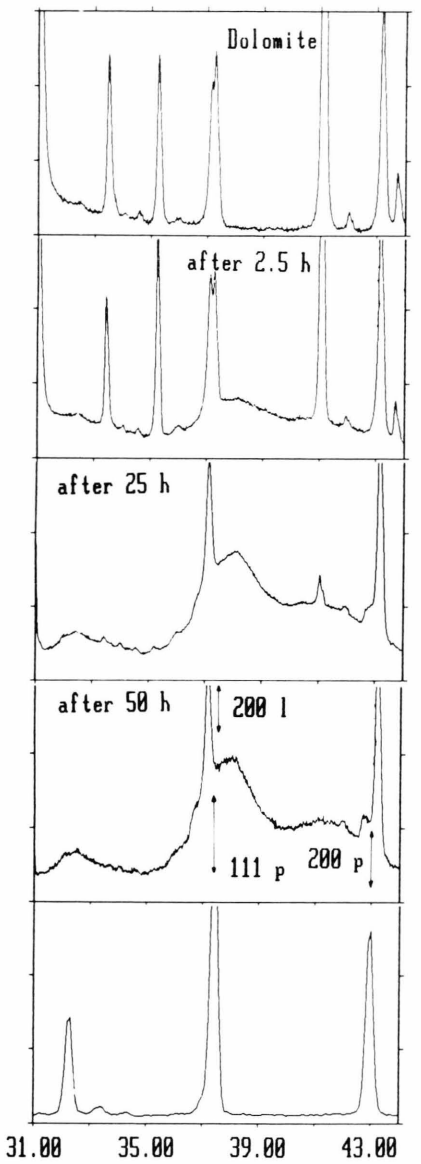

Fig. 2. Top to bottom: room temperature powder XRD patterns taken on the starting material, during the decomposition run C (C-2.5, C-25, C-50), and after heating of the final products at 1000 K. The vertical lines indicate the expected location of lime (l), periclase (p), and dolomite (d) XRD peaks.

with rock salt structure. Figure 2 shows the angular range relevant to the 111 and 200 lines of these products as recorded during experiment C (experiments A and B gave similar results). For the sake of comparison, the figure reports also part of the XRD patterns taken on the starting material,

and on the final products after heating at 1000 K for several days. It may be easily seen that the CaO lines are always very broad and correspond to a lattice parameter notably lower than the expected value: $a \sim 0.475$ nm, instead of $a = 0.4810$ nm. The peaks are very asymmetric and look as if they were made of at least two diffraction lines with slightly different locations. These features do not change with time, which obviously makes difficult an accurate evaluation of the time dependence of intensity: a (rough) estimate, however, shows in all experiments that a linear trend (passing through the origin) is followed, at least until the half reaction time is reached.

As for MgO, a more complex behaviour was found. First, it should be noted that sharp diffraction lines of this material were detected before the starting of the decomposition reaction and, to a lesser extent, even on the fresh sample at room temperature (see the top section of Figure 2). This has been ascribed both to the origin of the sample and to the onset of the half decomposition reaction when the sample temperature is raised under vacuum up to the final value. Rather surprisingly, the intensities of these lines do not grow during the reaction (see Fig. 2), but new lines appear, whose features are similar to those of the CaO lines, although with an abnormally high lattice parameter.

Experiments A and B indicated also the formation of calcite as a minor product. Indeed, two broad diffraction peaks (at $2\varnothing \sim 28.1°$ and $2\varnothing \sim 46.7°$, see Fig. 1) were assigned to the 10.4 and 10.8 lines (hexagonal indexes) of this structure, although showing locations significantly different from those pertinent to normal calcite (note that the difference cannot be explained by formation of a magnesian calcite). The intensity *vs* time plot is almost linear, without any induction period or saturation (Figure 3). Experiment C does not show calcite formation (Fig. 4): the different behaviour should be connected with the pressure, which is an order of magnitude lower than in experiment A, while the decomposition temperature is practically the same.

For the sake of completeness, a series of lines are finally to be mentioned, which occur in the $23° \leqq 2\varnothing \leqq 27°$ range of the patterns (see Figs. 1 and 4); they are evident also in the starting material and consequently are to be connected with the decomposition of some impurity.

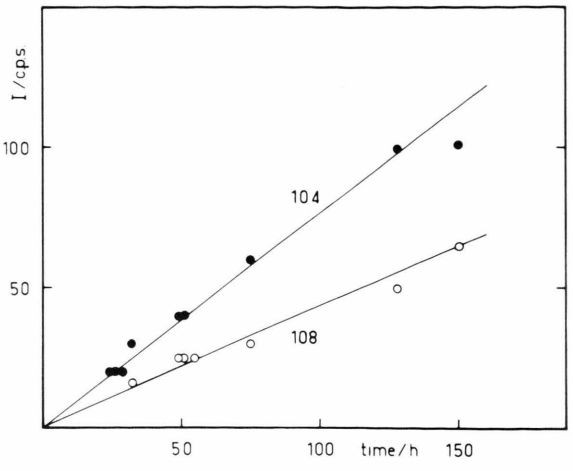

Fig. 3. Intensities of calcite XRD lines during the decomposition run B.

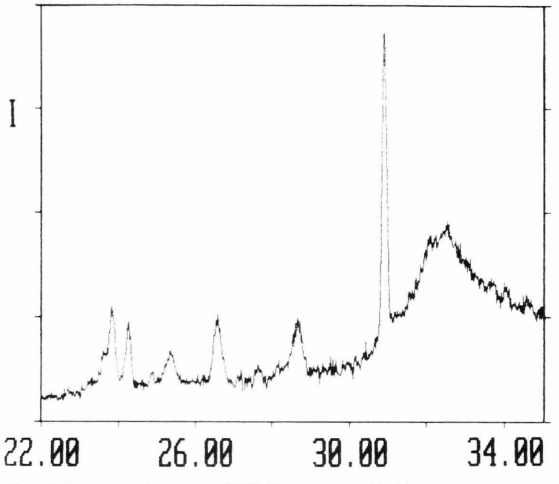

Fig. 4. Low angle part of XRD pattern C-50.

Discussion

The most significant result is the simultaneous formation of lime and periclase with small particle sizes and anomalous lattice spacings, respectively lower and higher than the established values. This suggests that what is actually produced is a pair of Ca-rich and Mg-rich solid solutions (Ca,Mg)O with the usual rock salt structure. A rough estimate of the composition of either solution gives (5–15%) deviations from stoichiometry, whereas the mutual solubilities of CaO and MgO are so low (at the

temperatures considered) that one should expect XRD patterns practically indistinguishable from those of pure lime and periclase.

During the thermal decomposition of dolomite, two different processes occur: the homogeneous and ordered solution of Ca and Mg cations is splitted into spatially distinct regions, and the carbonate anions decompose to oxide. We have already shown [1] that the former process cannot occur before the latter: they should occur simultaneously in a concerted manner or the latter should precede the former. Assuming that each phase produced by the various reactions is within the limits of its intrinsic stability, we are left with two possibilities:

a) full decomposition in a direct way, or

b) passage through half decomposition with three consecutive reactions:

b.1) half decomposition to magnesian calcite, periclase and carbon dioxide,

b.2) segregation of further MgO to produce a Mg-poorer calcite and

b.3) decomposition of this residual calcite *.

Moreover, we should indicate whether a nucleation and growth mechanism, or a shear mechanism is active in the relevant steps, *i.e.* either a), or b.1) to b.3).

A better understanding of dolomite full decomposition is gained by remarking the analogy with spinodal decompositions, a process whose first step gives a couple of metastable phases with spinodal composition whereas the equilibrium phases (with binodal composition) are produced in a further step by interdiffusion of structural elements. This seems to be our case too, with the difference that the diffusional movements are not active and the second step requires more drastic conditions.

In other words, the experimental evidence shows that the main step of dolomite full decomposition (in the low temperature and low pressure conditions investigated here) is a direct and diffusionless process.

Further arguments exist in favour of the above conclusion. First, it is worth remembering that – during decomposition – the MgO-rich phase does not produce any increase of the intensities of the previously formed MgO lines. This means that a diffusionless reaction is working, rather than a diffusion controlled growth of the preexistent crystallites.

Moreover, the linear trend of intensity *vs* time suggests that the kinetics of the rate-limiting step is the advancement of an interface of constant area, which is in agreement with a shear mechanism.

Another feature usually connected to a shear mechanism (when a large molar volume discrepancy exists between the crystal structures of reagents and products) is that small sized particles are formed over the whole reaction time, as their dimensions are determined by geometrical factors: indeed Fig. 5 shows that the line widths of the oxides remain constant during the reaction.

The above arguments are positively in favour of reaction (a); moreover, we can note that there is no experimental evidence either against (a), or in favour of the conflicting possibility (b), such as an induction time in the intensity *vs* time plots of the oxide lines, or a saturation behaviour in those of calcite.

Calcite formation itself, however, needs some explanatory remarks. In our opinion, calcite is formed by recarbonation of CaO due to a build up of carbon dioxide pressure within the porous microstructure of the direct products, so that the local

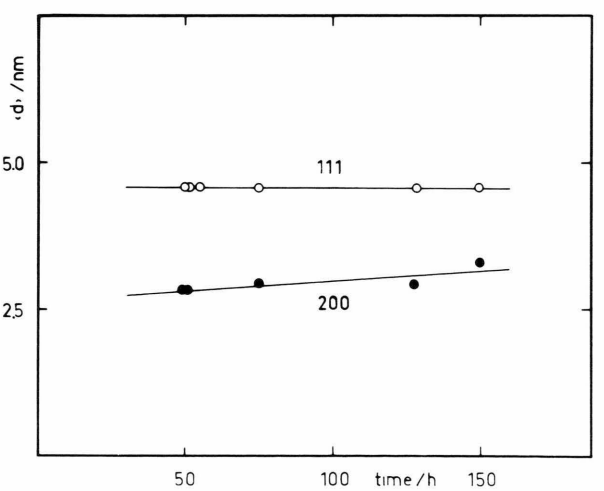

Fig. 5. CaO particle sizes during the decomposition run B, calculated with the Scherrer equation ($d \sim k\lambda/[B(2\varnothing)\cos\varnothing]$; $k = 1$), without instrumental broadening correction.

* Note that the relative extent of reactions b.1 – b.3 depends on how close they are to equilibrium: for example, if we assume that they are all quasi-equilibrium steps, it turns out that, at the temperature of the present experiments, reaction b.2 is practically irrelevant.

values of the thermodynamic variables are actually in a (T, P) region where direct oxide formation is possible but calcite decomposition is not. This opinion is in agreement both with the results of experiment C (where a lower value of the total external pressure is used and calcite is not formed) and with our thermodynamic model, which shows that such a (T, P) region does exist. Moreover, it can explain the already reported irregularities of the calcite phase. By making an approximate estimate of the lattice parameters, we obtained, at room temperature, $a = (0.548 \pm 0.015)$ nm and $c = (1.70 \pm 0.05)$ nm. The former is much higher, and the latter is practically coincident with the parameters of normal calcite (0.499 nm and 1.706 nm, respectively): note also that the anion-cation interlayer spacing (0.283 nm) is close to the value pertinent to the normal form of CaO (0.278 nm). This suggests that the calcite produced by recarbonation grows within the pores of the primary products in a kind of topotactic reaction and that its alternate cationic and anionic layers follow closely those of the CaO substrate, whereas the dimension of their hexagonal network is uniformly strained.

An unexpected result is that the amount of the calcite phase at the end of experiment A is a bit higher than at the end of experiment B. Note that, on purely thermodynamic grounds, at higher temperatures reactions b.1)–b.3) should be less favoured than reaction a). Again, this means that there is no direct competition between the reaction paths (a) and (b): calcite formation is kinetically controlled by the rate of direct oxide formation. In experiment A decomposition is faster than in experiment B; a larger carbon dioxide pressure is built up near the reaction interface, and, therefore, the formation of a larger amount of calcite may be justified.

Acknowledgements

The authors wish to thank A. W. Searcy for having kindly supplied the dolomite samples. One of us (G. S.) is also indebted to him for many helpful discussions on the subject of this work during a stay in Berkeley. This work was partly supported by M.P.I. (40% funds).

[1] G. Spinolo and D. Beruto, J. Chem. Soc., Faraday Trans. 1, **78,** 2631 (1982).
[2] E. K. Powell and A. W. Searcy, J. Amer. Ceram. Soc. **61,** 216 (1978).
[3] A. W. Searcy and D. Beruto, Nature London **263,** 271 (1976).
[4] A. W. Searcy and D. Beruto, J. Phys. Chem. **80,** 425 (1976), and **82,** 163 (1978); G. Bertran, J. Phys. Chem. **82,** 2536 (1978); A. W. Searcy and D. Beruto, J. Phys. Chem. **82,** 2537 (1978).
[5] G. Spinolo, V. Massarotti, and G. Campari, J. Phys. E: Sci. Instrum. **12,** 1059 (1979).
[6] G. Spinolo and U. Anselmi Tamburini, Internal Report (in Italian), Centro Studi C.N.R. and Dipartimento di chimica fisica, Universitá di Pavia, December 1983.